Extrapolated surface-wave dispersion inversion

Hongyu Sun and Laurent Demanet, Massachusetts Institute of Technology*

SUMMARY

We propose a surface-wave analysis method, extrapolated dispersion inversion (EDI), to image the near-surface shear-wave velocity structures beyond the penetration depth of conventional surface-wave inversion methods. Active-source surface waves are the main type of seismic data for an imaging depth of less than one kilometer. The relatively low-frequency data play an important role in dispersion inversion, by increasing the investigation depth and decreasing the inversion uncertainty. However, recorded surface-wave data from an active source generally lack low-frequency components below 3 Hz since acquiring them with an active-source survey requires considerable cost. Here, we propose to extrapolate the missing low-frequency surface waves from band-limited data so that low-frequency dispersion data can be measured. Due to the strong nonlinearity of bandwidth extension, we rely on deep learning to automatately extrapolate the missing low-frequency surface waves. Numerical examples with synthetic layered models show that the extrapolated data provide additional dispersion data at long wavelengths and thus can be used to image much deeper structures compared with inversion using only band-limited data.

INTRODUCTION

Rayleigh waves and Love waves propagate along the surface of the Earth and dominate the seismic recordings with strong energy. Instead of being taken as noise, surface waves have been used to image and characterize the near-surface shear-wave velocity structures with their dispersion property by assuming a horizontally layered (1D) medium (Dorman and Ewing, 1962; Nazarian et al., 1983; Xia et al., 1999; Park et al., 1999). More recently, Li et al. (2017, 2018); Liu et al. (2019); Zhang et al. (2021b) develop wave-equation inversion of dispersion data so that 2D or 3D velocity models with lateral heterogeneities are expected to be retrieved from surface waves.

Surface waves have the following advantages to image the subsurface. First, shallow sharp velocity contrasts cannot be readily captured with reflection-based methods or even acoustic full-waveform inversion (FWI) (Masclet et al., 2019). Moreover, compared with FWI, surface-wave dispersion inversion is less contaminated with the cycle-skipping problem and more time-efficient. It has been used to build initial models for FWI (Borisov et al., 2020).

Surface wave particle motion decreases with depth, which is dependent on the frequency of the waves. Larger wavelengths penetrate deeper for a given mode. Rix and Leipski (1995) examine the influence of the maximum wavelength contained in the dispersion curve on the accuracy of S-wave velocity profiles and find that the curve with the maximum wavelength yields the most accurate results at large depths; as the length of the maximum wavelength increases, the accuracy of the inverted profile in the intermediate layers also increases. Vantassel and Cox (2021) show that inversion uncertainty and non-uniqueness effects are minimal for simple subsurface models with broad-band dispersion data but cannot be ignored for more complex models characterized by band-limited dispersion data.

Low-frequency surface waves may be generated using very massive sources albeit at a considerable increase in the implementation cost (Foti et al., 2018). Regarding the impact of low frequencies on the investigation depth, Park et al. (1999) recommend always using a heavy impulsive source and low-frequency receivers with no recording filters. Extra processing is also required to enhance low-frequency signals. However, owing to the limitations in the bandwidth of regular geophones and sources, low frequencies below 3 Hz are generally missing from active-source surface-wave data. Conversely, passive sources in nature have sufficient energy down to very low frequencies, which make them appealing for the investigation of deep velocity structures (Park et al., 2005, 2007). For instance, Le Meur et al. (2020) retrieve low-frequency surface waves down to 0.5 Hz from interferometric virtual shot gathers and demonstrate the benefits of such low frequencies in velocity model building using a field dataset with a complex near-surface composition. The virtual data, however, are combined with higher frequencies from active data to ensure the accuracy of imaging the very-shallow velocity layers.

Recently, machine learning has been applied to surface-wave dispersion inversion in two aspects. Some researchers study automatic dispersion curve picking with deep learning (Alyousuf et al., 2018; Zhang et al., 2020; Ren et al., 2020; Kaul et al., 2020; Dai et al., 2021; Dong et al., 2021; Song et al., 2021; Ren et al., 2021) or other machine learning methods (Masclet et al., 2019; Rovetta et al., 2021; Wang et al., 2021; Yao et al., 2021). Others directly map surface-wave data to velocity models by performing surface-wave inversion with deep neural networks (Cheng et al., 2019; Hou et al., 2019; Hu et al., 2020; Zwartjes, 2020; Liu et al., 2021; Yablokov et al., 2021; Aleardi and Stucchi, 2021; Yang et al., 2021; Luo et al., 2022; Cai et al., 2022). Here we propose another application of deep learning for surface-wave inversion by extrapolating the low frequencies of surface waves so that deeper velocity structures can be imaged by surface-wave dispersion inversion.

Low-frequency extrapolation with deep learning was originally proposed for solving the cycle-skipping problem of FWI (Sun and Demanet, 2018, 2019, 2020b; Ovcharenko et al., 2019; Hu et al., 2021; Fabien-Ouellet, 2020; Jin et al., 2022; Zhao et al., 2020; Nakayama and Blacquière, 2021). A few field-data examples have verified the feasibility of data-driven bandwidth extension methods (Aharchaou and Baumstein, 2020; Wang et al., 2020; Fang et al., 2020; Zhang et al., 2021a). With supervised learning, neural networks are trained using pairs of

band-limited and low-frequency components of seismic data in the training data sets and then used to extrapolate the missing low frequencies for target areas. Although most studies work in the acoustic regime, Sun and Demanet (2020a) and Ovcharenko et al. (2020) propose methods to extrapolate the low frequencies of elastic data. Lin et al. (2021) and Robins et al. (2021) apply low-frequency extrapolation to electromagnetic scattered and medical ultrasound data, respectively. All these contributions aim at relieving the dependence of inversion on initial models, by leveraging the extrapolated low frequencies.

In this work, the motivation of low-frequency extrapolation of surface waves is to increase the investigation depth and to reserve the benefits of surface-wave inversion for near-surface imaging and characterization using active-source data. We therefore propose a surface-wave inversion method, extrapolated dispersion inversion (EDI), by including extrapolated low-frequency surface waves in dispersion curve picking. The extrapolated low frequencies give access to dispersion measurement at larger wavelengths and thus are expected to detect deeper structures. We use the deep-learning model proposed in Sun and Demanet (2022) to extrapolate the low frequencies from band-limited surface-wave data. Our numerical example using a synthetic layered-model data set illustrates the potential and benefits of increasing image depth with EDI.

METHOD AND DATA

We start by illustrating the important role of low frequencies in surface-wave inversion using a 1D layered model (Figure 1a). Figure 1b shows the sensitivity kernels of the fundamental mode calculated by taking the partial derivative of the dispersion velocities with respect to S-wave velocity of the model. With decreasing frequency, surface waves become sensitive to deeper velocity structures. The lower the frequency, the deeper the structure sampled. In particular, the layers below 300 m can only be detected using data below 2 Hz. However, acquiring such low frequencies with an active source is impractical or uneconomical. Instead, computationally extrapolating from band-limited data is a much cheaper way to obtain a reasonable approximation to low-frequency surface waves.

Low-frequency extrapolation with deep learning

A crucial step of EDI is low-frequency extrapolation of band-limited surface waves. We use the deep-learning model (Figure 2) in Sun and Demanet (2022) to extrapolate low frequencies from band-limited surface-wave data. We train the neural network in a supervised fashion with pairs of low-frequency and band-limited time series. The input of the neural network is a group of three band-limited traces recorded by adjacent receivers. The output of the neural network is the low-frequency counterpart of the middle trace of the input.

We demonstrate the workflow of EDI and the performance of low-frequency extrapolation with deep learning using a synthetic data set simulated on a collection of horizontally layered models. With a regular grid spacing of 2.5 m, each model is 500 m in depth and 1000 m in width. The number of lay-

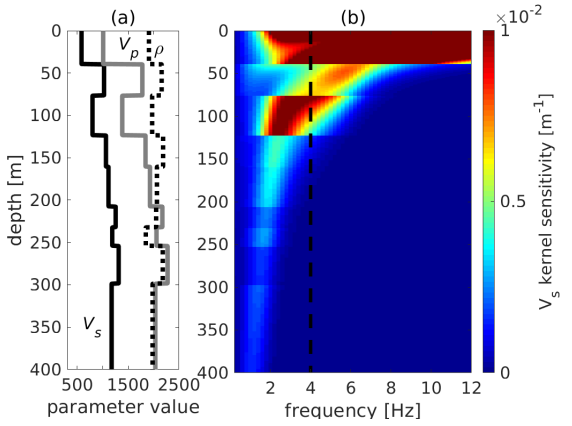

Figure 1: (a) 1D subsurface model described in terms of S-wave velocity (V_s, [m/s]), P-wave velocity (V_p, [m/s]), and density (ρ, [kg/m^3]). (b) Sensitivity kernels with respect to V_s of the fundamental mode. The penetration depth increases with the decrease of frequency. In particular, the layers below 300 m can only be detected using data below 2 Hz.

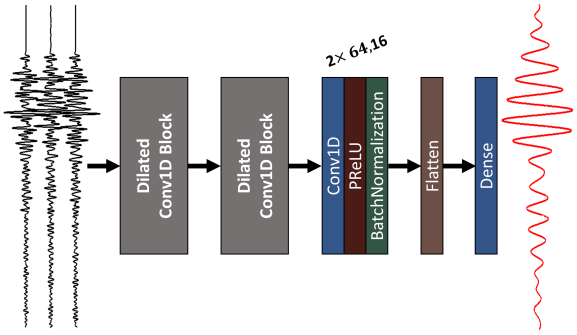

Figure 2: Deep learning architecture for low-frequency extrapolation. The model uses a kernel length of 2 on all 1D convolutional layers and employs exponential dilation rates to efficiently increase the receptive field of the convolutional neural network. Details can be found in Sun and Demanet (2022).

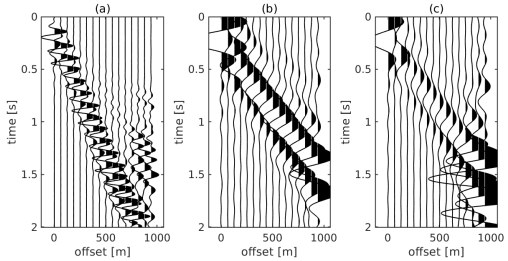

Figure 3: Extrapolation results of test model in Figure 1: Comparison of surface waves in vertical components in (a) $4-15$ Hz band-limited, (b) extrapolated low-frequency, and (c) true low-frequency shot gather below 4 Hz.

ers on each model is random and follows an uniform distribution $n \backsim U(3,14)$. The thickness (th) and S-wave velocity of each layer are randomly sampled from $th \backsim U(20,50)$ m, and $V_s \backsim U(500,1000)$ m/s, respectively. In addition, we ensure that velocities generally increase with depth by adding a velocity of $[500(i-1)]/(n-1)$ m/s to the random velocity of the i-th layer. The deepest layer is considered the half-space, and its thickness is extended to the end of the model. Poisson's ratio is fixed for these models, and we use 1.732 as the ratio of V_p/V_s. The density is also fixed with 1800 kg/m^3. With this model building method, we generate 500 models in total and use 400 models as training models, 30 models as validation models and the rest as test models.

The surface waves are simulated using the open-source finite-difference code SOFI2D (Bohlen, 2002; Bohlen and Saenger, 2006) with a free-surface boundary condition on the top of each model. The source wavelet is a Ricker wavelet with a dominant frequency of 10 Hz. We simulate only one shot on each layered model. The shot gather contains Rayleigh waves recorded by 401 vertical-component geophones with an interval of 2.5 m. The sampling rate and recording length are 0.002 s and 2 s, respectively. The maximum offset is 1000 m. The raw shot gather is preprocessed trace-by-trace by first normalizing to one by its maximum and then multiplying by a constant of 100. After prepossessing, each full-band trace is split into low-frequency time series below 4 Hz and band-limited counterparts above 4 Hz. With every three band-limited traces as one sample, the 401 traces of one shot are split into 399 samples for training. In total, the training data set contains $399 \times 70 = 27,930$ samples. Both low-frequency and band-limited time series are downsampled with a factor of 2 before being fed into the neural network. Thus the dimension is 500×3 for the input and 500×1 for the output. After training, we trace-by-trace predict the low frequencies for a test model and then combine all traces based on their offsets to generate one low-frequency shot gather.

Extrapolated dispersion inversion

Following bandwidth extension, we can construct a pseudo full-band shot gather containing surface waves by combining extrapolated low frequencies with band-limited data. Then we calculate the Rayleigh waves phase velocity dispersion image using the Phase-Shift method (Park et al., 1998). With the extrapolated low-frequency data, we can pick additional dispersion curve of the fundamental mode at long wavelengths from the pseudo full-band dispersion image. Combining the dispersion curve of an extended frequency range with the existing band from active surface waves attempts to increase the maximum depth of V_s estimation.

Profiles of Earth's parameters can be derived from dispersion data with various inversion methods. Here the inversion engine is a perturbational method based on finite elements and is implemented using the RAYLEE package (Haney and Tsai, 2017). The initial model for the iterative inversion is calculated by a Dix-type nonperturbational inversion method (Haney and Tsai, 2015). We parametrize the subsurface model with only the S-wave velocity and thickness of each layer. The P-wave velocity and density inside each layer are derived from V_s for the forward problem. This simplified parametrization does not impact the solution in a significant way as Rayleigh waves are mostly sensitive to V_s (Xia et al., 1999).

RESULTS

We extrapolate low-frequency surface waves from band-limited shot records on test models using the neural network trained with 10 epochs. Figure 3 compares the $4-15$ Hz band-limited data, extrapolated and true low-frequency data below 4 Hz on the test model in Figure 1. Traces with a regular spacing of 62.5 m are plotted among the 399 traces of one shot gather. Overall the extrapolated data match the true low frequencies except events with later arrival time and far offsets. After reconstructing pseudo full-band shot gathers, we compare the amplitude spectra of the entire shot gather with extrapolated and true low frequencies (Figure 4). The low-frequency components below 4 Hz are recovered although they are completely missing before extrapolation. The difference between two amplitude spectra shows that the extrapolation accuracy decreases with decreasing frequencies and increasing offsets. At a relatively far offset of 800 m, errors of the amplitude spectra are around 10 dB.

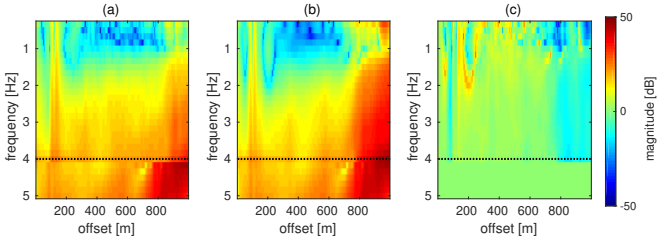

Figure 4: Extrapolation results of test model in Figure 1: Comparison of amplitude spectrum between data with (a) extrapolated and (b) true low frequencies below 4 Hz. (c) The difference between data with extrapolated and true low frequencies.

We then calculate the dispersion data using all traces of one shot gather. The dispersion image with $0.5-4$ Hz extrapolated data generally match that with $0.5-4$ Hz true data (Figure 5), which implies that the trained neural network captures the dispersion property of surface waves in addition to extrapolating low frequencies. However, the small-scale discontinuity around 4 Hz suggests that the accuracy of the extrapolated data is not perfect. Further research improving the performance would be to modify the neural network and training strategies according to the physical property of surface waves.

Dispersion curves are picked from the dispersion images as the input measurements for surface-wave inversion (Figure 5). Figure 6 compares the resulting dispersion curves (inverted using $4-14$ Hz band-limited and $0.5-14$ Hz full-band data with true or extrapolated $0.5-4$ Hz low frequencies) with the measurements. All the inverted dispersion curves meet the picked ones in their frequency ranges. The EDI resulting V_s profile roughly aligns with the profile inverted using $0.5-14$ Hz full-band data (Figure 7). However, the inverted profile using $4-14$ Hz band-limited data loses constraints in

the deep region below 150 m, which is conforming to the sensitivity kernel (Figure 1). In contrast, despite discrepancies in the middle layers, EDI with $0.5-4$ Hz extrapolated data can detect the deepest layers accurately. The difference highlights the impact of low-frequency information on dispersion inversion. Moreover, since we did not invert sharp profiles using dispersion data, we evaluate the inversion results by comparing the inverted profiles with the true model after smoothing. The inverted profiles with either true or extrapolated low frequencies is comparable with the true profile after smoothing except the minor errors (less than 50 m/s) in the intermediate depth. This simple example indicates that EDI is potentially an attractive solution to the problem of insufficient detection depth of surface-wave inversion with active-source data.

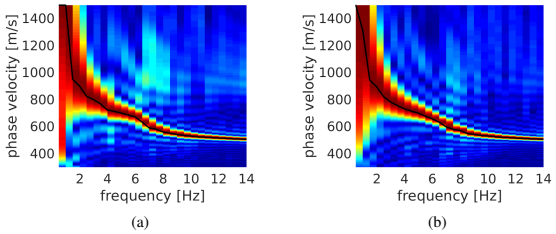

Figure 5: Dispersion images of data with $0.5-4$ Hz (a) extrapolated and (b) true low frequencies. Black lines denote dispersion curves of fundamental mode picked from panels.

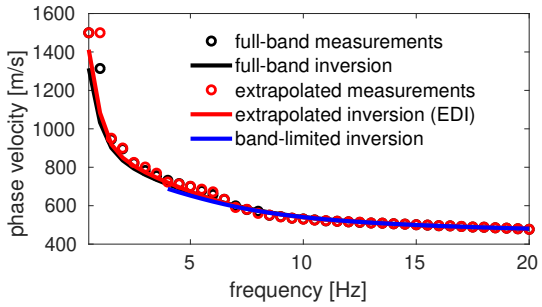

Figure 6: Inversion results for the test model in Figure 1: Comparison of the inverted and measured dispersion curves.

DISCUSSION

There are several limitations with the method. First, EDI requires reliable low-frequency extrapolation of surface waves, which depends on successful training and generalization of the deep neural networks. Although the neural network did not see the test model during training, the training and test models are from the same data distribution in our example. Future work on out-of-sample testing is important to study the generalization for surface-wave extrapolation. Second, we speculate that only a few frequencies around the lower band of band-limited data could be reliably extrapolated, owing to the intrinsic nature of surface-wave dispersion. Even so, we can expect an increase of several times of the investigation depth if the minimum frequency of the band-limited data is low as

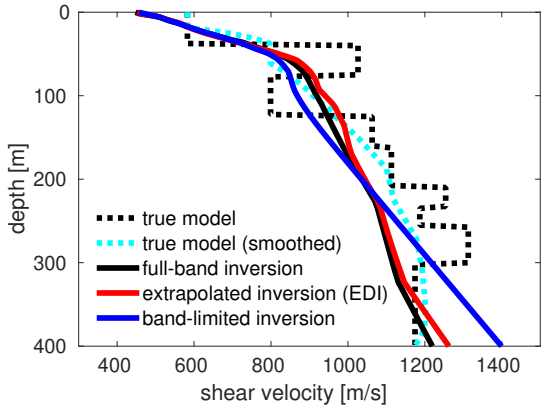

Figure 7: Inversion results for the test model in Figure 1: Comparison of inverted V_s profiles with the true model. The EDI result (red line) roughly aligns with the result using $0.5-14$ Hz full-band data (solid black line), and can detect the deep layer below 300 m more accurate than that using $4-14$ Hz band-limited data (blue line).

the penetration depth is inversely proportional to the minimum frequency. Thrid, EDI may be inappropriate for dealing with higher modes since overtones generally appear at relatively high-frequency ranges for field data. In our example, we only pick the fundamental mode using the extrapolated low frequencies. In addition, the problem of non-unique solutions may arise when several sets of parameters yield the same dispersion curve. However, EDI could in principle reduce the inversion uncertainties thanks to extra constraints in the extrapolated frequency range.

CONCLUSION

By extrapolating low-frequency components from band-limited surface waves, EDI incorporates additional dispersion data at long wavelengths for increasing the detection depth of surface-wave analysis. When extrapolating with sufficient accuracy, EDI enables us to achieve deeper near-surface characterization than surface-wave inversion with band-limited data. The synthetic example using layered models is encouraging and shows its potential to deal with field surface-wave data. Although we focus on Rayleigh waves in this work, the proposed method is also applicable to other kinds of surface waves, such as Love and Scholte waves, which however require specific forward modeling algorithms and data acquisition procedures.

ACKNOWLEDGMENTS

The authors acknowledge MIT MathWorks Science Fellowship and MIT Earth Resources Laboratory for funding. The authors thank Niels Grobbe, Robert D. van der Hilst, and Liguo Han for helpful discussion.

REFERENCES

Aharchaou, M., and A. Baumstein, 2020, Deep learning-based artificial bandwidth extension: Training on ultrasparse OBN to enhance towed-streamer FWI: The Leading Edge, **39**, 718–726.

Aleardi, M., and E. Stucchi, 2021, A hybrid residual neural network - Monte Carlo approach to invert surface wave dispersion data: Near Surface Geophysics, **19**, 397–414.

Alyousuf, T., D. Colombo, D. Rovetta, and E. Sandoval-Curiel, 2018, Near-surface velocity analysis for single-sensor data: An integrated workflow using surface waves, AI, and structure-regularized inversion, *in* SEG Technical Program Expanded Abstracts 2018: Society of Exploration Geophysicists, 2342–2346.

Bohlen, T., 2002, Parallel 3-D viscoelastic finite difference seismic modelling: Computers & Geosciences, **28**, 887–899.

Bohlen, T., and E. H. Saenger, 2006, Accuracy of heterogeneous staggered-grid finite-difference modeling of Rayleigh waves: Geophysics, **71**, T109–T115.

Borisov, D., F. Gao, P. Williamson, and J. Tromp, 2020, Application of 2D full-waveform inversion on exploration land data: Geophysics, **85**, R75–R86.

Cai, A., H. Qiu, and F. Niu, 2022, Semi-supervised surface wave tomography with Wasserstein cycle-consistent GAN: Method and application to Southern California plate boundary region: Journal of Geophysical Research: Solid Earth, e2021JB023598.

Cheng, X., Q. Liu, P. Li, and Y. Liu, 2019, Inverting Rayleigh surface wave velocities for crustal thickness in eastern Tibet and the western Yangtze craton based on deep learning neural networks: Nonlinear Processes in Geophysics, **26**, 61–71.

Dai, T., J. Xia, L. Ning, C. Xi, Y. Liu, and H. Xing, 2021, Deep learning for extracting dispersion curves: Surveys in Geophysics, **42**, 69–95.

Dong, S., Z. Li, X. Chen, and L. Fu, 2021, DisperNet: An effective method of extracting and classifying the dispersion curves in the frequency-Bessel dispersion spectrum: Bulletin of the Seismological Society of America, **111**, 3420–3431.

Dorman, J., and M. Ewing, 1962, Numerical inversion of seismic surface wave dispersion data and crust-mantle structure in the New York-Pennsylvania area: Journal of Geophysical Research, **67**, 5227–5241.

Fabien-Ouellet, G., 2020, Low-frequency generation and denoising with recursive convolutional neural networks, *in* SEG Technical Program Expanded Abstracts 2020: Society of Exploration Geophysicists, 870–874.

Fang, J., H. Zhou, Y. Elita Li, Q. Zhang, L. Wang, P. Sun, and J. Zhang, 2020, Data-driven low-frequency signal recovery using deep-learning predictions in full-waveform inversion: Geophysics, **85**, A37–A43.

Foti, S., F. Hollender, F. Garofalo, D. Albarello, M. Asten, P.-Y. Bard, C. Comina, C. Cornou, B. Cox, G. Di Giulio, et al., 2018, Guidelines for the good practice of surface wave analysis: a product of the InterPACIFIC project: Bulletin of Earthquake Engineering, **16**, 2367–2420.

Haney, M. M., and V. C. Tsai, 2015, Nonperturbational surface-wave inversion: A dix-type relation for surface waves: Geophysics, **80**, EN167–EN177.

———, 2017, Perturbational and nonperturbational inversion of Rayleigh-wave velocities: Geophysics, **82**, F15–F28.

Hou, S., S. Angio, A. Clowes, I. Mikhalev, H. Hoeber, and S. Hagedorn, 2019, Learn to invert: Surface wave inversion with deep neural network: 81st EAGE Conference and Exhibition 2019 Workshop Programme, European Association of Geoscientists & Engineers, 1–5.

Hu, J., H. Qiu, H. Zhang, and Y. Ben-Zion, 2020, Using deep learning to derive shear-wave velocity models from surface-wave dispersion data: Seismological Research Letters, **91**, 1738–1751.

Hu, W., Y. Jin, X. Wu, and J. Chen, 2021, Progressive transfer learning for low-frequency data prediction in full waveform inversion: Geophysics, **86**, 1–82.

Jin, Y., W. Hu, S. Wang, Y. Zi, X. Wu, and J. Chen, 2022, Efficient progressive transfer learning for full-waveform inversion with extrapolated low-frequency reflection seismic data: IEEE Transactions on Geoscience and Remote Sensing, **60**, 1–10.

Kaul, A., A. Abubakar, A. Misbah, and P. J. Bilsby, 2020, Detecting the fundamental mode of energy for surface wave analysis, modelling, and inversion, using a deep convolutional network, *in* SEG Technical Program Expanded Abstracts 2020: Society of Exploration Geophysicists, 1571–1575.

Le Meur, D., D. Donno, J. Courbin, D. Solyga, and A. Prescott, 2020, Retrieving ultra-low frequency surface waves from land blended continuous recording data, *in* SEG Technical Program Expanded Abstracts 2020: Society of Exploration Geophysicists, 1855–1859.

Li, J., Z. Feng, and G. Schuster, 2017, Wave-equation dispersion inversion: Geophysical Journal International, **208**, 1567–1578.

Li, J., S. Hanafy, and G. Schuster, 2018, Wave-equation dispersion inversion of guided P waves in a waveguide of arbitrary geometry: Journal of Geophysical Research: Solid Earth, **123**, 7760–7774.

Lin, Z., R. Guo, M. Li, A. Abubakar, T. Zhao, F. Yang, and S. Xu, 2021, Low-frequency data prediction with iterative learning for highly nonlinear inverse scattering problems: IEEE Transactions on Microwave Theory and Techniques, **69**, 4366–4376.

Liu, L., Y. Liu, T. Li, Y. He, Y. Du, and Y. Luo, 2021, Inversion of vehicle-induced signals based on seismic interferometry and recurrent neural networks: Geophysics, **86**, Q37–Q45.

Liu, Z., J. Li, S. M. Hanafy, and G. Schuster, 2019, 3D wave-equation dispersion inversion of Rayleigh waves: Geophysics, **84**, R673–R691.

Luo, Y., Y. Huang, Y. Yang, K. Zhao, X. Yang, and H. Xu, 2022, Constructing shear velocity models from surface wave dispersion

curves using deep learning: Journal of Applied Geophysics, **196**, 104524.

Masclet, S., T. Bardainne, V. Massart, and H. Prigent, 2019, Near surface characterization in Southern Oman: Multi-wave inversion guided by machine learning: 81st EAGE Conference and Exhibition 2019, European Association of Geoscientists & Engineers, 1–5.

Nakayama, S., and G. Blacquière, 2021, Machine-learning-based data recovery and its contribution to seismic acquisition: Simultaneous application of deblending, trace reconstruction, and low-frequency extrapolation: Geophysics, **86**, P13–P24.

Nazarian, S., K. H. Stokoe II, and W. R. Hudson, 1983, Use of spectral analysis of surface waves method for determination of moduli and thicknesses of pavement systems: Transportation Research Board, 38–45.

Ovcharenko, O., V. Kazei, M. Kalita, D. Peter, and T. Alkhalifah, 2019, Deep learning for low-frequency extrapolation from multioffset seismic data: Geophysics, **84**, R989–R1001.

Ovcharenko, O., V. Kazei, P. Plotnitskiy, D. Peter, I. Silvestrov, A. Bakulin, and T. Alkhalifah, 2020, Extrapolating low-frequency prestack land data with deep learning, *in* SEG Technical Program Expanded Abstracts 2020: Society of Exploration Geophysicists, 1546–1550.

Park, C., R. Miller, N. Rydén, J. Xia, and J. Ivanov, 2005, Combined use of active and passive surface waves: Environmental and Engineering Geophysics, **10**, 323–334.

Park, C. B., R. D. Miller, and J. Xia, 1998, Imaging dispersion curves of surface waves on multi-channel record, *in* SEG Technical Program Expanded Abstracts 1998: Society of Exploration Geophysicists, 1377–1380.

———, 1999, Multichannel analysis of surface waves: Geophysics, **64**, 800–808.

Park, C. B., R. D. Miller, J. Xia, and J. Ivanov, 2007, Multichannel analysis of surface waves (MASW) active and passive methods: The Leading Edge, **26**, 60–64.

Ren, L., F. Gao, P. Williamson, and G. A. McMechan, 2021, On application issues of automatic dispersion curves picking by machine learning: First International Meeting for Applied Geoscience & Energy, Society of Exploration Geophysicists, 1836–1840.

Ren, L., F. Gao, Y. Wu, P. Williamson, W. Wang, and G. A. McMechan, 2020, Automatic picking of multi-mode dispersion curves using CNN-based machine learning, *in* SEG Technical Program Expanded Abstracts 2020: Society of Exploration Geophysicists, 1551–1555.

Rix, G. J., and E. A. Leipski, 1995, Accuracy and resolution of surface wave inversion: Recent Advances in Instrumentation, Data Acquisition and Testing in Soil Dynamics, ASCE, 17–32.

Robins, T., J. Camacho, O. C. Agudo, J. L. Herraiz, and L. Guasch, 2021, Deep-learning-driven full-waveform inversion for ultrasound breast imaging: Sensors, **21**, 4570.

Rovetta, D., A. Kontakis, and D. Colombo, 2021, Application of a density-based spatial clustering algorithm for fully automatic picking of surface-wave dispersion curves: The Leading Edge, **40**, 678–685.

Song, W., X. Feng, G. Wu, G. Zhang, Y. Liu, and X. Chen, 2021, Convolutional neural network, Res-Unet++, -based dispersion curve picking from noise cross-correlations: Journal of Geophysical Research: Solid Earth, **126**, e2021JB022027.

Sun, H., and L. Demanet, 2018, Low frequency extrapolation with deep learning, *in* SEG Technical Program Expanded Abstracts 2018: Society of Exploration Geophysicists, 2011–2015.

———, 2019, Extrapolated full waveform inversion with convolutional neural networks, *in* SEG Technical Program Expanded Abstracts 2019: Society of Exploration Geophysicists, 4962–4966.

———, 2020a, Elastic full-waveform inversion with extrapolated low-frequency data, *in* SEG Technical Program Expanded Abstracts 2020: Society of Exploration Geophysicists, 855–859.

———, 2020b, Extrapolated full-waveform inversion with deep learning: Geophysics, **85**, R275–R288.

———, 2022, Deep learning for low-frequency extrapolation of multicomponent data in elastic FWI: IEEE Transactions on Geoscience and Remote Sensing, **60**, 1–11.

Vantassel, J. P., and B. R. Cox, 2021, SWinvert: A workflow for performing rigorous 1-D surface wave inversions: Geophysical Journal International, **224**, 1141–1156.

Wang, M., S. Xu, and H. Zhou, 2020, Self-supervised learning for low frequency extension of seismic data, *in* SEG Technical Program Expanded Abstracts 2020: Society of Exploration Geophysicists, 1501–1505.

Wang, Z., C. Sun, and D. Wu, 2021, Automatic picking of multi-mode surface-wave dispersion curves based on machine learning clustering methods: Computers & Geosciences, **153**, 104809.

Xia, J., R. D. Miller, and C. B. Park, 1999, Estimation of near-surface shear-wave velocity by inversion of Rayleigh waves: Geophysics, **64**, 691–700.

Yablokov, A. V., A. S. Serdyukov, G. N. Loginov, and V. D. Baranov, 2021, An artificial neural network approach for the inversion of surface wave dispersion curves: Geophysical Prospecting, **69**, 1405–1432.

Yang, J., C. Xu, and Y. Zhang, 2021, A new mathematical model for dispersion of Rayleigh wave and a machine learning based inversion solver: arXiv preprint arXiv:2106.14025.

Yao, H., W. Cao, X. Huang, and B. Wu, 2021, Automatic extraction of surface wave dispersion curves using unsupervised learning: First International Meeting for Applied Geoscience & Energy, Society of Exploration Geophysicists, 1826–1830.

Zhang, H., P. Yang, Y. Liu, Y. Luo, and J. Xu, 2021a, Deep learning-based low-frequency extrapolation and impedance inversion of seismic data: IEEE Geoscience and Remote Sensing Letters (early access, doi: 10.1109/LGRS.2021.3123955).

Zhang, X., Z. Jia, Z. E. Ross, and R. W. Clayton, 2020, Extracting dispersion curves from ambient noise correlations using deep learning: IEEE Transactions on Geoscience and Remote Sensing, **58**, 8932–8939.

Zhang, Z.-d., E. Saygin, L. He, and T. Alkhalifah, 2021b, Rayleigh wave dispersion spectrum inversion across scales: Surveys in Geophysics, **42**, 1281–1303.

Zhao, T., A. Abubakar, X. Cheng, and L. Fu, 2020, Augment time-domain FWI with iterative deep learning, *in* SEG Technical Program Expanded Abstracts 2020: Society of Exploration Geophysicists, 850–854.

Zwartjes, P., 2020, Near surface velocity estimation from phase velocity-frequency panels with deep learning: EAGE 2020 Annual Conference & Exhibition Online, European Association of Geoscientists & Engineers, 1–5.